

The Influence of Substrate Material on the Thermal Cycling Fatigue Life of Thermal Barrier Coating Systems

Robert Eriksson^{1,a}, Håkan Brodin^{1,2,b}, Sten Johansson^{1,c}, Lars Östergren^{3,d}
and Xin-Hai Li^{2,e}

¹ Linköpings universitet, IEI, 58183 Linköping, Sweden

² Siemens Industrial Turbomachinery AB, 61283 Finspång, Sweden

³ Volvo Aero Corporation, 46181 Trollhättan, Sweden

^a robert.eriksson@liu.se, ^b hakan.brodin@liu.se, ^c sten.johansson@liu.se,

^d lars.g.ostergren@volvo.com, ^e xin-hai.li@siemens.com

Keywords: TBC, thermal barrier coating, thermal cycling fatigue, fractography, substrate material, interdiffusion, oxidation

Abstract. Thermal barrier coatings (TBCs) are used in gas turbines to provide insulation against high temperature and to provide oxidation and corrosion resistance for the superalloys on which they are deposited. TBCs are deposited on hot parts in the combustor and on the turbine blades, and must consequently be compatible with the various superalloys used there. The influence of substrate material on the durability of TBCs has therefore been studied. Air plasma sprayed TBCs have been deposited on Hastelloy X and Haynes 230, which are alloys used in the combustor. The TBC systems have been thermally cycled until failure and their fracture surfaces have been studied. The thermally grown oxides and the substrate/coating interdiffusion have also been analysed by energy dispersive spectroscopy. The fatigue life, fracture mechanism and the oxide composition and kinetics were similar for the two TBC systems; however, one of the TBC systems is thought to have failed prematurely.

Introduction

Thermal barrier coating (TBC) systems are commonly used in gas turbines to provide protection against high-temperature degradation and oxidation of the substrate materials [1]. TBCs consist of a metallic bond coat (BC) and a ceramic top coat (TC) deposited on the substrate by methods such as air plasma spray (APS) and electron beam physical vapour deposition (EB-PVD) [1,2]. The APS process, which is used in this study, gives rise to a splat-on-splat microstructure, shown in Fig. 1. The contact between layers of splats may be low, and there consequently exists delaminations (voids) between the splats, shown in Fig. 1.

The bond coat is often chosen among the MCrAlY alloys where M is Ni and/or Co. The bond coat provides oxidation resistance through the formation of alumina [3]; the bond coat also enables proper adhesion of the APS top coat. The top coat is made of yttria partially stabilised zirconia (Y-PSZ) and provides the desired thermal insulation.

As the TBC system is thermally cycled, the difference in coefficient of thermal expansion (CTE) between the various components in the TBC system causes stresses in the interface regions [4,5] and the TBC system eventually fails by fatigue. Rigs of various designs have been developed to test the thermal cyclic fatigue life of TBC systems, such as furnace cycling rigs and burner rigs [6,7]. Thermal cycling of TBCs in such rigs will cause the top coat to spall off; the fracture surface will

appear dark or bright depending on whether the fracture occurred in the BC/TC interface or in the TC; these two types of fracture is therefore referred to as black and white fracture respectively [5,6]. Most common is that a single fracture surface possesses both types [5].

Another mechanism of failure is through the formation of thermally grown oxides (TGOs) in the BC/TC interface. When the aluminium reservoir in the bond coat is depleted, oxides other than protective alumina may become common among the TGOs in the BC/TC interface; as they are generally non-protective, and may introduce cracking due to growth stresses, they may cause failure of the TBC [3,8].

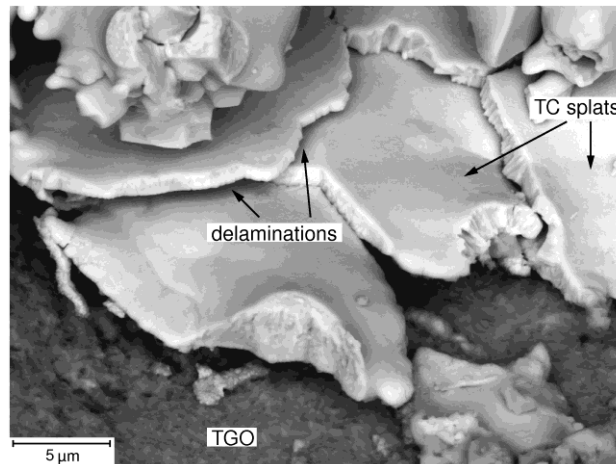


Fig. 1. Air plasma sprayed top coat (TC) on top of a layer of thermally grown oxides (TGO).

Previous Work. The influence of the substrate material on the thermal fatigue life of TBCs is yet to be fully understood; some attention is currently being given to the subject. Previous studies on the influence of substrate material on TBC life includes Wu et al. [9] and Wu and Reed [10] who tested the thermal cycling life of TBC systems on several substrates and found that the substrate material did influence fatigue life; the suggested explanation was changes in fracture toughness of the BC/TGO interface.

Schulz et al. [11] and He et al. [12] studied the fatigue life of TBCs on various single crystal and directionally solidified substrates. The single crystals generally gave the shortest TBC fatigue life and several explanations were suggested for this. Some features of the single crystals, which may have contributed to shorter TBC life, were: they were generally higher in refractory elements; they were generally lower in C, B and Cr; they developed large pores at the substrate/BC interface; they had a larger CTE mismatch with the BC; they developed a wavy TGO. However, the studied single crystals did not necessarily have the fastest oxidation kinetics.

Schulz et al. [11] also found that directionally solidified alloys, which had longer lives, gave a TGO with pegs that extended into the bond coat. Such pegs were often rich in Hf, and Hf was consequently suggested to prolong TBC life.

Pint et al. [13] studied the influence of Y and S concentrations in a single crystal substrate on the thermal fatigue life of EB-PVD TBC. De-sulphurised substrates, as well as sulphur-containing substrates with Y additions, gave longer fatigue lives.

While it is quite clear that the thermal fatigue life of TBCs is influenced by the substrate material, not enough attention has so far been given to this subject, and, particularly, no attention has been given to air plasma sprayed TBC systems on typical combustor materials; previous studies have dealt mainly with EB-PVD TBCs on blade materials.

Therefore, the influence of two wrought combustor materials on the thermal fatigue life of air plasma sprayed TBCs has been studied. The specimens have been thermally cycled to failure, and the fracture surfaces have been studied. In addition, cross-sectioned specimens have been used to study oxidation of the bond coat, and interdiffusion between the substrate and bond coat.

Experimental

TBC systems, deposited on two different substrate materials, were exposed to thermal cycling fatigue (TCF). The TBC systems consisted of 150 μm of air plasma sprayed Ni-Co-Cr-Al with minor additions of Y, Ta, and Si, and 1.5 mm of air plasma sprayed 7 % yttria partially-stabilised zirconia. The substrate materials were Hastelloy X and Haynes 230, which were disc-shaped with a radius of 25 mm and a thickness of 5 mm. The major element additions of the composition of the substrates are given in Table 1. The two specimens will hereafter be referred to as HX and H230, for TBC on Hastelloy X and Haynes 230 respectively.

Table 1. Compositions of the substrate materials.

	Ni	Cr	W	Fe	Mo	Co	Mn	Al	C	
Hastelloy X	balance	22	0.6	18	9	1	0.5	—	0.1	[wt.%]
Haynes 230	balance	22	14	1.5	1.3	0.4	0.6	0.3	0.1	[wt.%]

The specimens were thermally cycled between 100 $^{\circ}\text{C}$ and 1100 $^{\circ}\text{C}$; the hold time at high temperature was 1 h, and the cooling to low temperature was done by forced air flow during 10 min. The specimens were cycled until the top coat spalled off completely, which allowed the fracture surfaces to be studied. Such fractographic studies were done in a stereo microscope and a Hitachi SU-70 field emission gun scanning electron microscope (SEM).

In addition to the thermal cycling fatigue, two additional specimens (one of each configuration) were isothermally oxidised at 1100 $^{\circ}\text{C}$ for 500 h. They were then cross-sectioned, mounted and polished, and were used for establishing the TGO thickness, and for interdiffusion studies by energy dispersive spectroscopy (EDS).

Results and Discussion

Thermal Cycling Fatigue. The TCF lives and TGO thicknesses are reported in Table 2. The TCF lives of the two TBC systems were in the same order of magnitude; however, the H230 specimen is thought to have failed prematurely; other experiences with this TBC system suggests the life to be considerable longer than the life reported here. Since the premature failure enabled the two TBC systems to be compared after roughly the same high-temperature exposure, the results of the fractography were considered interesting nonetheless.

The TGO thickness after 500h at 1100 $^{\circ}\text{C}$ was essentially the same for the two specimens, and the difference in TCF life is thus not due to any major differences in oxidation kinetics.

Table 2. The thermal fatigue lives and oxide thicknesses of the specimens.

Specimen	TCF life, [cycles]	TGO thickness after 500 h of isothermal oxidation, [μm]
HX	565	6.2
H230	501*	6.5

* premature failure

Fractography. Fig. 2 shows the two fracture surfaces (BC side and TC side) of the failed H230 specimen. The black areas on the BC side of the fracture surface, Fig. 2 a), are areas where the fracture has occurred in the BC/TC interface, whereas the white areas are fracture in the top coat; the two types of fracture are referred to as black and white fracture.

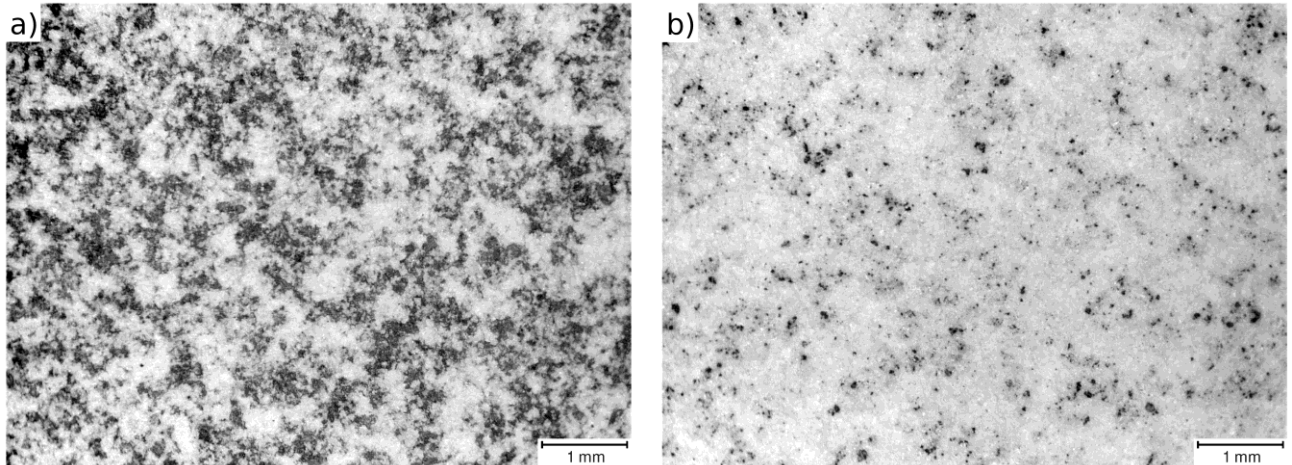


Fig. 2. Fracture surfaces from failed thermally cycled TBCs. The images are from stereo microscopy of the H230 specimen. a) The bond coat side of the fracture. b) The top coat side of the fracture.

The amount of black fracture on the two specimens has been established by image analysis made on images from stereo microscopy on the BC side of the fracture surface, Fig. 2 a). The HX specimen consisted of 39.4 % and H230 of 33.7 % black fracture. The difference is perhaps not large enough to be attributed to any major difference in fracture mechanism; however, stereo microscopy do give the impression that the H230 specimen has failed somewhat further away from the BC/TC interface, (further into the top coat), hence the somewhat lower amount of black fracture.

The dark spots on the TC side of the fracture surface, Fig. 2 b), are TGOs which have detached from the interface TGO layer. The amount of TGOs on the TC side of the fracture surface can be used to conclude how large fraction of the black fracture that occurred in the BC/TGO interface or in the TGO, rather than in the TGO/TC interface. For HX the amount of TGO on the TC side of the fracture surface was 4.9 %, and for H230 3.3 %; or, recalculated as fraction of the black fracture: the black fracture consisted of 12.4 % and 9.8 % BC/TGO or in-TGO fracture for HX and H230 respectively.

To summarise: the HX, compared to H230, had a slightly higher percentage black fracture and the black fracture did, to a larger extent, consist of BC/TGO or in-TGO fracture. However, the difference was not all that large, and the fracture behaviour was rather similar for the two specimens, although not identical.

Fig. 3 shows a comparison between the fracture surfaces of the two TBC systems. The images are backscatter electron SEM images of the BC side of the fracture surfaces. The bright areas are residues of the top coat, and the darker gray and black areas are the exposed interfacial TGOs. On a micro-scale level, the two specimens appear to have fractured in a very similar manner.

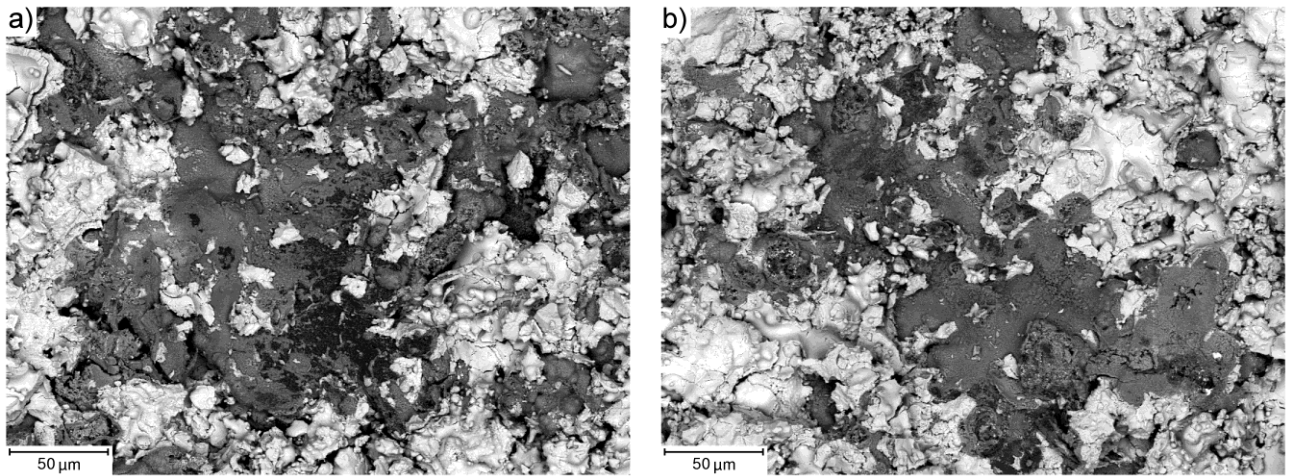


Fig. 3. Scanning electron microscopy images showing the fracture surfaces in comparison: a) bond coat side of specimen HX, b) bond coat side of specimen H230.

In areas of white fracture, the fracture has occurred mainly in the pre-existing delaminations between the splats (shown in Fig. 1), leaving a quite smooth fracture surface. Fig. 4 a) shows such a fracture where the splats have detached at pre-existing delaminations, without breaking individual splats. This behaviour is observed for both substrate materials; this has been shown to be a common way of failure for the TC [14–16].

In the areas of black fracture, the TGO layer appears to be rather unharmed. As discussed earlier, the black fracture is made up of mostly TGO/TC fracture (~ 90 %). Most of the exposed TGO is continuous without any extensive cracking, and the top coat appears to have separated rather cleanly from the bond coat, as shown in Fig. 4 b). Again, on a micro-scale level, the fracture mechanism appears to be similar for the two TBC systems studied here.

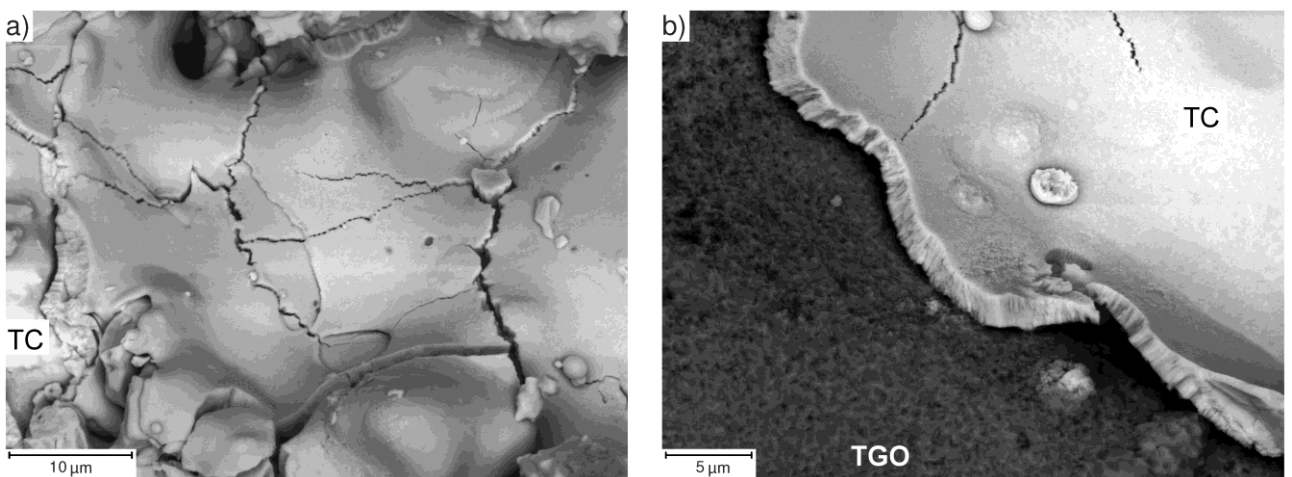


Fig. 4. Electron images from the fracture surfaces. a) Fracture in the top coat in specimen HX. b) Fracture in the interface of thermally grown oxides (TGO) and the top coat (TC), in specimen H230.

Oxidation and Interdiffusion. For simplicity, the oxides found on the fracture surface may be divided into three groups based on their morphology and composition, they are all shown in Fig. 5:

1) alumina, containing essentially just Al and O; 2) a thin layer of granular oxides on top of the alumina, they are rich in Al, but also contains significant amounts of Cr, Ni and Co; 3) blocky oxides rich in chromium, with significant amounts of Ni and Co and lower amounts of Al. The later two may be spinels or chromia. An overview of the oxides on the fracture surface is provided by Fig. 6, which is an EDS map of the elements most commonly found in the oxides.

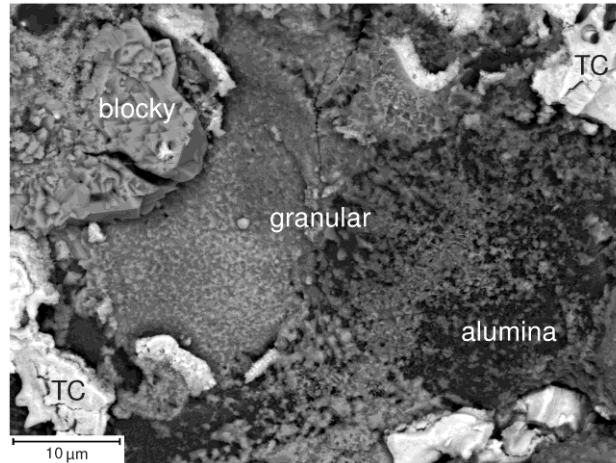


Fig. 5. Electron image showing the various types of oxides, distinguishable by their corresponding morphology and composition; image from the bond coat side of the fracture surface of specimen H230.

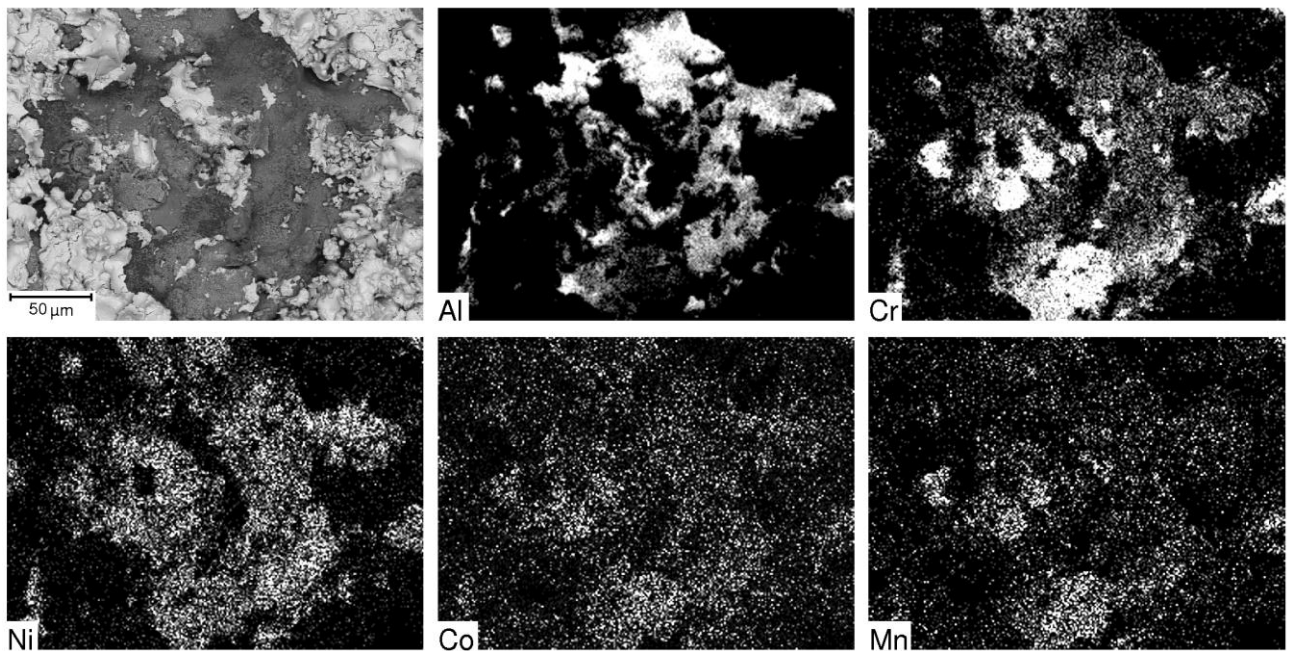


Fig. 6. EDS maps showing an overview of the thermally grown oxides visible on the fracture surfaces. Image shows the bond coat side of the fracture surface of specimen H230.

The oxides found on the fracture surfaces were analysed by EDS. The occurrence of substrate alloying elements (W, Fe, Mo, Mn) is of special interest since they diffuse into the bond coat and might partake in the oxide formation in the BC/TC interface.

No W and Mo were found in the TGOs on the fracture surfaces. Mn, on the other hand, was found in the TGO, and it appears to favour oxides high in Cr and low in Al: the alumina contains no detectable Mn; granular oxides, which still are rich in Al, contain 0.6–1.1 at.% Mn; and the blocky oxides, which are rich in Cr, contain 2–2.7 at.% Mn. This can also be seen in the EDS map in Fig. 6 where the Mn concentration is higher in the Cr rich blocky oxides.

The TGOs of the HX specimen contain somewhat higher Mn (the higher end of the intervals previously given) than H230 (the lower end of the intervals). Minor amounts of Fe was detected in some cases, most notably in the blocky oxides, which in HX contained 0.4 at.% and in H230 0.13 at.% Fe.

Fig. 7 shows the interdiffusion of substrate alloying elements into the bond coat; the element concentrations just beneath the TGO are printed out in numbers to facilitate the reading of the graph. It can be seen that Mn, which takes part in the formation of TGOs, is present in essentially the same amount in both specimens. Of the refractory elements Mo appears to interdiffuse quite readily, while W is present in considerably lower amounts at the BC/TGO interface; The TGO appears to act as an effective barrier for these elements, as none of them were found in the fracture surface TGOs.

As in previous studies made on EB-PVD TBCs on turbine blade materials [9–13], the interdiffusion changes the chemistry at the BC/TGO interface, but do not necessarily change the TGO composition or growth kinetics. Contrary to previous studies, the TBC systems studied here failed at the TGO/TC interface rather than the BC/TGO interface. Many of the previously suggested mechanisms for substrate material influence [9–13] focus on phenomena in the BC/TGO interface. In this study, the BC/TGO chemistry is different for the two substrate materials, but the fracture still occurs at the TGO/TC interface, and previously suggested mechanisms may not sufficiently explain the influence of substrate material in this case.

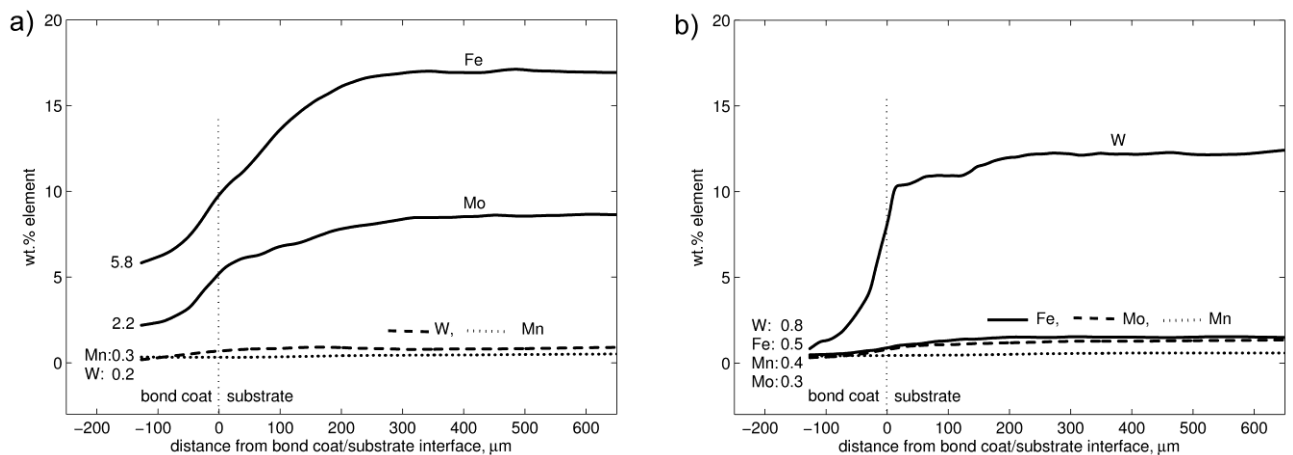


Fig. 7. Elemental profiles showing substrate/bond coat interdiffusion after 500 h oxidation at 1100 °C. The numbers at the start of each curve indicates the element concentration in the bond coat just below the TGOs. a) Hastelloy X b) Haynes 230

Conclusions

The thermal cycling fatigue life of TBCs deposited on two different substrates, Hastelloy X and Haynes 230, was studied. The results may be summarised as:

- The lives, in this study, are in the same order of magnitude, although the H230 specimen is thought to have failed prematurely.
- HX has a slightly larger fraction black fracture, and a larger fraction of the black fracture is BC/TGO or in-TGO fracture rather than TGO/TC fracture.
- The BC/TGO interface of the HX specimen contains higher amounts of substrate elements which have diffused into the bond coat, most notably Mo and Fe.
- The TGOs of the two specimens are similar in thickness and composition.
- Of the substrate elements, Mn, and to a lesser extent Fe, reach the TGO/TC interface where it partition to mixed-element oxides. HX has a somewhat higher Mn content in the TGOs.

Previously suggested explanations for the substrate influence on fatigue life [9–13] may not be applicable here since the fracture occurred in the TGO/TC interface rather than in the BC/TGO interface. It is unfortunate that the H230 specimen failed prematurely; however, continued testing will provide more information on the damage development during thermal cycling, and the possible effects of substrate material on fatigue life, for these TBC systems.

Acknowledgement

This research has been funded by the Swedish Energy Agency, Siemens Industrial Turbomachinery AB, Volvo Aero Corporation, and the Royal Institute of Technology through the Swedish research programme TURBO POWER, the support of which is gratefully acknowledged. The authors would also like to accentuate the contribution of Professor Sören Sjöström.

References

- [1] X. Zhao and P. Xiao: Mater. Sci. Forum Vol. 606 (2009), p. 1
- [2] R. Vassen, A. Stuke and D. Stöver: J. Therm. Spray Technol. Vol. 18 (2009), p. 181
- [3] A. Rabiei and A.G. Evans: Acta Mater. Vol. 48 (2000), p. 3963
- [4] S. Sjöström and H. Brodin, in: Advanced Ceramic Coatings and Interfaces V, edited by, D. Zhu and H.-T. Lin, volume 31 of Ceramic Engineering and Science Proceedings, issue, 3, John Wiley & Sons, Inc. (2010)
- [5] H. Brodin: *Failure of thermal barrier coatings under thermal and mechanical fatigue loading: Microstructural observations and modelling aspects* (Linköpings universitet, Sweden 2004)
- [6] R. Eriksson, H. Brodin, S. Johansson, L. Östergren and X.-H. Li: Surf. Coat. Technol. Vol. 205 (2011), p. 5422
- [7] R. Vassen, F. Cernushi, G. Rizzi, A. Scriveri, N. Markocsan, L. Östergren, A. Kloosterman, R. Mevrel, J. Feist and J. Nicholls: Adv. Eng. Mater. Vol. 10 (2008), p. 907
- [8] W.R. Chen, X. Wu, B.R. Marple and P.C. Patnaik: Surf. Coat. Technol. Vol. 197 (2005), p. 109
- [9] R.T. Wu, K. Kawagishi, H. Harada and R.C. Reed: Acta Mater. Vol. 56 (2008), p. 3622
- [10] R.T. Wu and R.C. Reed: Acta Mater. Vol. 56 (2008), p. 313
- [11] U. Schulz, M. Menzebach, C. Leyens and Y.Q. Yang: Surf. Coat. Technol. Vol. 146-147 (2001), p. 117
- [12] L. He, Z. Xu, J. Li, R. Mu, S. He and G. Huang: J. Mater. Sci. Technol. Vol. 25 (2009), p. 799
- [13] B.A. Pint, I.G. Wright, W.Y. Lee, Y. Zhang, K. Prüssner and K.B. Alexander: Mater. Sci. Eng., A Vol. 245 (1998), p. 201
- [14] R. Eriksson, H. Brodin, S. Johansson, L. Östergren and X.-H. Li: Procedia Eng. Vol. 10 (2011), p. 195
- [15] P.D. Harmsworth and R. Stevens: J. Mater. Sci. Vol. 27 (1992), p. 616
- [16] E. Wessel and R.W. Steinbech: Key Eng. Mater. Vol. 223 (2002), p. 55